ARMY RESEARCH LABORATORY

Growth of Low Defect Density Gallium Nitride (GaN) Films on Novel Tantalum Carbide (TaC) Substrates for Improved Device Performance

by M. A. Derenge, K. A. Jones, K. W. Kirchner, T. S. Zheleva, and R. D. Vispute

ARL-TR-4818 **May 2009**

NOTICES

Disclaimers

The findings in this report are not to be construed as an official Department of the Army position unless so designated by other authorized documents.

Citation of manufacturer's or trade names does not constitute an official endorsement or approval of the use thereof.

Destroy this report when it is no longer needed. Do not return it to the originator.

Army Research Laboratory
Adelphi, MD 20783-1197

ARL-TR-XXX **May 2009**

Growth of Low Defect Density Gallium Nitride (GaN) Films on Novel Tantalum Carbide (TaC) Substrates for Improved Device Performance

M. A. Derenge, K. A. Jones, K. W. Kirchner, and T. S. Zheleva
Sensors and Electron Devices Directorate, ARL

R. D. Vispute
Bluewave, Incorporated
Physics Department, U. of Maryland
College Park, MD 20742

REPORT DOCUMENTATION PAGE	Form Approved OMB No. 0704-0188

PLEASE DO NOT RETURN YOUR FORM TO THE ABOVE ADDRESS.

1. REPORT DATE *(DD-MM-YYYY)*	2. REPORT TYPE	3. DATES COVERED (From - To)
May 2009	Final	

4. TITLE AND SUBTITLE	5a. CONTRACT NUMBER
Growth of Low Defect Density Gallium Nitride (GaN) Films on Novel Tantalum Carbide (TaC) Substrates for Improved Device Performance	5b. GRANT NUMBER
	5c. PROGRAM ELEMENT NUMBER

6. AUTHOR(S)	5d. PROJECT NUMBER
M. A. Derenge, K. A. Jones, K. W. Kirchner, T. S. Zheleva, and R. D. Vispute	5e. TASK NUMBER
	5f. WORK UNIT NUMBER

7. PERFORMING ORGANIZATION NAME(S) AND ADDRESS(ES)	8. PERFORMING ORGANIZATION REPORT NUMBER
U.S. Army Research Laboratory ATTN: AMSRD-ARL-SE-RL 2800 Powder Mill Road Adelphi, MD 20783-1197	ARL-TR-XXX

9. SPONSORING/MONITORING AGENCY NAME(S) AND ADDRESS(ES)	10. SPONSOR/MONITOR'S ACRONYM(S)
	11. SPONSOR/MONITOR'S REPORT NUMBER(S)

12. DISTRIBUTION/AVAILABILITY STATEMENT

Approved for public release; distribution unlimited.

13. SUPPLEMENTARY NOTES

14. ABSTRACT

To potentially improve device performance, we attempted to grow gallium nitride (GaN) films with better crystalline quality (fewer mismatch dislocations) using a tantalum carbide (TaC) substrate, which is more closely lattice matched to GaN than currently used substrates. We created the TaC substrate, using pulse laser deposition (PLD) of TaC onto (0001) SiC substrates at ~1000 °C, and grew GaN films, using metal organic chemical vapor deposition (MOCVD). Using x-ray diffraction, we determined the TaC films grown on-axis were higher quality than the off-axis films, but the latter could be improved to a comparable quality by annealing at 1200–1600 °C for 30 min. We also deposited GaN films onto the TaC after it had been nitrided with NH_3 for 3 min at 1100 °C and used aluminum nitride (AlN) as a low temperature nucleation layer. Using these methods, the crystalline quality of the GaN films was higher—the grains were ~10 times larger than those typically seen in films grown on SiC or sapphire, and they contained more than an order of magnitude fewer dislocations compared to a typical value of 4×10^9 cm^{-2}. However, the grains lacked the required (0001) texture, producing a very rough surface.

15. SUBJECT TERMS

tantalum carbide, gallium aluminum nitride, silicon carbide, lattice match

16. SECURITY CLASSIFICATION OF:			17. LIMITATION OF ABSTRACT	18. NUMBER OF PAGES	19a. NAME OF RESPONSIBLE PERSON
a. REPORT	b. ABSTRACT	c. THIS PAGE			M. E. Derenge
Unclassified	Unclassified	Unclassified	UU	34	19b. TELEPHONE NUMBER (*Include area code*) (301) 394-1195

Contents

List of Figures iv

List of Tables v

1. Introduction 1

2. Experimental Procedure 5

3. Results and Discussion 6

4. Conclusions 21

5. References 22

List of Symbols, Abbreviations, and Acronyms 23

Distribution List 25

List of Figures

Figure 1. Schematic of the close packed structure of the growth plane and its three possible positions, A, B, or C.....2

Figure 2. Schematic of a Schottky diode structure (a) grown on an insulating substrate such as sapphire that requires front side contacts. This causes current crowding as shown by the red current lines, and (b) with a back side contact that eliminates current crowding and other related problems, such as premature breakdown.....3

Figure 3. SEM micrographs of TaC films (a) as-deposited at 800 °C, (b) deposited at 800 °C and annealed at 1200 °C, (c) deposited at 800 °C and annealed at 1600 °C, and (d) deposited 1000 °C and annealed at 1600 °C.....7

Figure 4. SEM micrographs of a TaC film deposited on an on-axis substrate at 1000 °C taken (a) at a high magnification and (b) in a region where micropores were observed.....8

Figure 5. The 5 x 5 μm AFM micrographs of TaC films deposited on an on-axis substrate at 1000 °C, showing (a) an as-deposited film and (b) a film that was annealed at 1400 °C. 8

Figure 6. A complete θ–2θ scan for a TaC film deposited at 1000 °C on an on-axis 6H-SiC substrate. 9

Figure 7. The θ–2θ scan for a TaC film deposited at 1000 °C in the vicinity of the (a) (111) TaC peak and (b) the (222) peak for the as-deposited and annealed films.....10

Figure 8. The θ–2θ scan for TaC films as-deposited at 1000 °C in the vicinity of (a) the (111) TaC peak and (b) the (222) peak for the on on-axis, 3° off-axis, or 8° off-axis films. The θ - 2θ scan for TaC films as-deposited at 1000 °C and annealed at 1600 °C in the vicinity of (c) the (111) TaC peak and (d) the (222) peak for the on-axis, 3° off-axis, or 8° off-axis films. Peaks 1 and 3 are extra peaks that could be associated with Ta_2C; the $(0002)_{GaN}$, $(111)_{TaC}$ and $(0006)_{SiC}$ peaks lie in region 2; and 4 is the $(200)_{TaC}$ peak. 11

Figure 9. The Debye ring pattern for the TaC film deposited at 1000 °C on a 3° off-axis substrate: (a) as-grown and (b) annealed at 1600°C with a GaN film grown on top of it. 12

Figure 10. (a) Cross section TEM micrograph of a TaC film grown at 1100 °C, and (b) the associated SAD pattern from a region near the TaC/6H-SiC interface. 13

Figure 11. (a) Cross section TEM micrograph of a TaC film grown at 1200 °C, (b) HRTEM of the same region, (c) HRTEM micrograph of a reaction product at the interface, and (d) SAD pattern of the associated area. 14

Figure 12. SEM micrographs of a GaN film grown for 45 min (a) away from the exposed SiC spot, and (b) near it. (c) SEM micrograph of a GaN film grown for 10 min.....16

Figure 13a. (a) A complete θ–2θ scan for a GaN film grown on a TaC film deposited at 1000 °C on a 3° off-axis SiC substrate. 17

Figure 13b. Rocking curve for the $(0004)_{GaN}$ and (222) peaks.....18

Figure 14. (a) Cross section TEM of a GaN film grown on a TaC film PLD deposited on a 4H-SiC substrate. (b) Cross section TEM of the GaN film and its associated SAD pattern and the TaC/GaN interface. 19

Figure 15. SEM images of GaN grown on (a) TaC and (b) the SiC “spot” at the same magnification, and (c) on the SiC spot at higher magnification. 20

List of Tables

Table 1. A comparison of important parameters used in selecting a substrate for the growth of GaN films. 4

INTENTIONALLY LEFT BLANK.

1. Introduction

High electron mobility transistors (HEMTs) made from gallium nitride (GaN) have the potential to handle more than five times the power at Ka-band (26.5–40 GHz) wavelengths than those made from gallium arsenide (GaAs), which are currently being used. This would enable radar systems to detect objects at more than twice the distance. Diodes and transistors made from GaN have the potential to operate more efficiently than silicon carbide (SiC) devices and be fabricated at a lower cost. This would enable hybrid electric vehicles to operate more efficiently and/or do so at a lower cost.

Unfortunately, these devices do not function nearly as well as they theoretically could because the GaN material contains many crystalline defects. Many of these defects are created during growth on a hetero-structural substrate, because large-area GaN wafers with good crystalline quality do not yet exist. Large-diameter GaN crystals have not been grown, because the vapor pressure of nitrogen (N) in equilibrium with GaN is so large at reasonable growth temperatures (*1*). As a result, researchers have used different substrates, such as SiC (*2,* 3) or sapphire (Al_2O_3) (*4,* 5), for growth on the basal (0001) plane, which is the only plane that will be considered in this report.

In addition to the substrate being a single crystal, the film and substrate being chemically compatible, and the ability of the substrate to survive in the growth environment for the film, the two critical parameters for choosing the substrate are its effective lattice parameter, a_0, and its crystal structure. The a_0 for the substrate should be as close as possible to that of the film to minimize the mismatch dislocation density, which is proportional to the square of the mismatch. The crystal structure of the substrate should be as similar as possible to that of the film to insure epitaxy; that is, the film will everywhere grow with the same orientation so it, too, will be a single crystal or at least an aggregate in which all the grains have the same orientation. The most important aspects of the crystal structure are how the atoms are arranged in the growth plane, how the planes parallel to the growth plane are stacked on top of each other, and how the atoms are bonded to each other. For this report we consider only the close packed (111) cubic or (0001) hexagonal planes, which are equivalent and are displayed in figure 1. One can visualize them as six hard spheres in contact with each other forming a hexagon around a seventh sphere at the center. Atoms lying in these positions form an “A” plane; when the atoms lie in the **B** interstice, they form a “B” plane; and when they lie in the **C** interstice, they form a “C” plane.

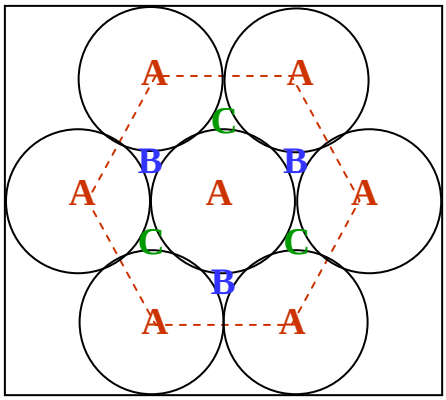

Figure 1. Schematic of the close packed structure of the growth plane and its three possible positions, A, B, or C.

The most common polytype of SiC used for the growth of GaN is 6H-SiC, and its a_0 = 0.3081 nm, which results in a –3.42% mismatch, given that a_0 for GaN = 0.3189 nm. For some applications, the ternary, aluminum gallium nitride (AlGaN), is preferred to GaN, and its a_0 decreases linearly with the Al concentration. Being negative, the mismatch decreases as the Al concentration increases, but even at 100% Al, the mismatch is still 1.01% as a_0(AlN) = 0.3112 nm. The molecular structure of SiC is also similar to GaN in that the atoms are tetrahedrally coordinated with sp^3 bonding, but the crystal structure differs in that the packing sequence for the close packed basal planes for 6H-SiC is AαBβCγAαCγBβ compared to the AαBβ packing for GaN. The Roman letters signify a layer of silicon atoms and the Greek letters signify a layer of carbon atoms; for the Aα sequence, the carbon atom lies directly on top of the silicon atom, not in one of the interstices. SiC also has the advantage that it can be made conducting by heavily doping it, which is useful for vertical high power devices. It can also be made insulating by growing it in a very pure state, which is useful for lateral high frequency devices. Furthermore, it has a high thermal conductivity, 4.9 W/cm·°C, so it can conduct heat away from these devices that often operate with a high power density.

The mismatch between GaN and Al_2O_3 is much larger. Assuming that the effective a_0 for Al_2O_3 is the distance between the Al atoms “almost” in the basal plane, which is 0.2808 nm, the mismatch is –11.95%. We use the word, “almost,” because every other Al atom is ~0.5 Å above the plane, while the alternate Al atoms are the same distance below. In addition, every third Al site is vacant. The planar distortion is created by the vacancies, which, in turn, are caused by the fact that the mole fraction of Al in Al_2O_3 is only 40%. In the idealized structure the small Al ions lie in ⅔ of the octahedral sites of this close packed structure, so the packing sequence of these close packed planes is Aγ′Bα′Cβ′; the (′) is used to indicate that ⅓ of the sites are vacant. In the actual structure the octahedra containing the Al ions are slightly distorted so that instead of being equidistant from the six oxygen ions that surround it, the Al-O bond lengths for three of the bonds is 0.186 nm, while for the other three it is 0.197 nm. In addition to its poor structural match-up with GaN, sapphire is an insulator, so that vertical devices with back side contacts

cannot be fabricated using it as a substrate. As shown in figure 2, this is a requirement to eliminate current crowding in high power devices, as they require thick epitaxial layers to achieve large breakdown voltages. It enables the use of a single backside contact that is often used in GaAs/AlGaAs optical emitter and detector arrays. Also, Al_2O_3 is a poor thermal conductor—the thermal conductivity is 0.2721 W/cm·°C.

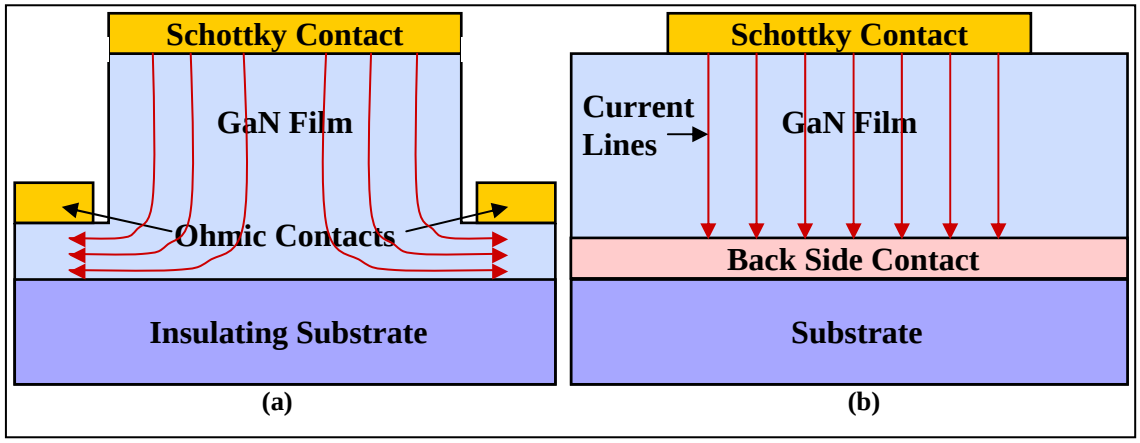

Figure 2. Schematic of a Schottky diode structure (a) grown on an insulating substrate such as sapphire that requires front side contacts. This causes current crowding as shown by the red current lines, and (b) with a back side contact that eliminates current crowding and other related problems, such as premature breakdown

With an effective lattice parameter of 0.3150 nm, tantalum carbide (TaC) is more closely lattice matched to GaN (1.24%), all of the octahedral holes in the face centered cubic (FCC) Ta lattice are filled with carbon (C) so that its AγBαCβ structure is not distorted, and it is conductive with a resistivity of only 25 μΩ·cm (*6*). Only its relatively small thermal conductivity of 0.221 W/cm·°C (*6*) appears to be a problem. The Ta–C system has the additional advantage that in the other tantalum-carbon stoichiometric compound, Ta_2C, the Ta basal plane has the close packed structure with C occupying every other octahedral site. With a_0 = 0.3104 nm, this ABγ hexagonal close packed (HCP) structure is more closely lattice matched to SiC. Thus, we could break the 3.42% lattice mismatch between the GaN into steps, SiC → Ta_2C (0.74%); Ta_2C → TaC (1.46%); and TaC → GaN (1.24%). Since the strain goes as the square of the mismatch, digitizing the mismatch between SiC and GaN could significantly reduce the strain in the GaN, thereby improving the structural quality of the GaN films. One could also reduce the strain further by eliminating the mismatch with the TaC by growing $Al_{.51}Ga_{.49}N$ on it, which is a composition of interest for ultraviolet (UV) emitters and detectors.

To circumvent the poor lattice mismatch and possibly the poor chemical compatibility between the GaN and the SiC or Al_2O_3 substrate, there are two steps we can take. First, we nitride the surface by heating it to ~1100 °C for a few minutes in ammonia (NH_3) in an metal organic chemical vapor deposition (MOCVD) system (*2*, *4*) or by exposing it to an N_2 flux for a few minutes at ~700 °C in a molecular beam epitaxy (MBE) reactor (*3*, *5*). Next we deposit a thin (30–80 nm) polycrystalline $Al_XGa_{1-X}N$ buffer layer, where *x* can range from 0 to 1. It is believed

that this buffer layer is able to somewhat reduce the mismatch strain, while still retaining epitaxial conditions. It is not, however, able to eliminate the effects of the lattice mismatch so that a high density of dislocations is formed, usually in the 10^9–10^{10} cm^{-2} range. The quality of the films grown on SiC are virtually the same as that achieved using sapphire substrates even though the bond structure of SiC is more similar to that of GaN and the lattice mismatch is smaller. Apparently, increasing the lattice mismatch beyond a critical value has little effect. The hope is that the small mismatch with the TaC is below that critical value so that it will provide a benefit. Also, if any chemical compatibility issues arise with the TaC, we should be able to deposit an AlGaN buffer layer on it, given that the carbon at or near the surface can be removed by heating the TaC in H_2 (*6*), and the Ta can be nitrided by heating it in NH_3 (*7*).

Table 1 shows a comparison of the different substrates to GaN (blue), where green represents the best choice, orange the middle choice, and red the worst choice. In this comparison, TaC is favored over SiC for its better lattice match, but is favored over Al_2O_3 in a number of aspects. TaC is only shown to be a poor choice for thermal conductivity, and even there the difference is very small. Note also that GaN sublimates (shown in red), which is why other substrates must be used.

Table 1. A comparison of important parameters used in selecting a substrate for the growth of GaN films.

Material	Mismatch %	Al % for Lattice Match	Coordination	Electrical Conductivity (mhos/cm)	Thermal Conductivity ($W/cm^2 \cdot °C$)	Melting Point (°C)
GaN	0	0	tetrahedral	variable	2.8	sublimates
SiC	–3.42 (O)	X (R)	tetrahedral (G)	variable (G)	4.9 (G)	2830 (O)
Al_2O_3	–11.95 (R)	X (R)	distorted (R) octahedral	insulator (R)	0.272 (O)	2054 (R)
TaC	–1.24 (G)	51 (G)	octahedral (O)	4×10^4 (O)	0.221 (R)	3983 (G)

Given that TaC is a chemically robust material with a very high melting point (3983 °C), and it is in equilibrium with SiC in the Si-Ta-C ternary phase diagram (*8*) suggesting chemical compatibility, one must ask the following questions:

1. Is TaC reactive enough so that, if necessary, the surface carbon can be removed and the Ta nitrided?
2. Even if it can be nitrided, will the surface be chemically active enough so that epitaxy can take place?
3. Given the high melting point of TaC, is there a method for preparing a single crystal substrate without growing a bulk crystal and cutting wafers from it?

Given that GaN films have been grown on titanium carbide (TiC) by MOCVD (*9*) and TaC has been deposited epitaxially on SiC substrates by pulse laser deposition (PLD) (*10*) and on magnesium oxide (MgO) substrates by electron beam evaporation (*11*), using TaC films effectively may be possible.

In this report we explore to what extent TaC films can be deposited epitaxially on SiC substrates using PLD and to what extent GaN films can be grown epitaxially on the TaC. Our process involved depositing TaC films at various temperatures onto on-axis and 3° and 8° off-axis SiC substrates, followed by growing GaN films on the TaC using MOCVD for various times on substrates subjected to different pre-treatments. We then examined the morphology of the TaC and GaN films using scanning electron microscopy (SEM) and atomic force microscopy (AFM), and studied their structure using x-ray diffraction (XRD), transmission electron microscopy (TEM), and high resolution TEM (HRTEM).

2. Experimental Procedure

Samples 8 x 6 mm in size were cut from SiC wafers that were on-axis, 3° 20″, or 8° 3″ off-axis, and TaC films 200–500 nm thick were deposited on them by PLD at temperatures ranging from 300–1200 °C using a krypton fluoride (KrF) (λ = 248 nm, τ = 20 ns) for the ablation of a stoichiometric TaC (99.995% purity) target. The laser energy density for the ablation was ~5 J/cm^2, and the pulse repetition rate was 10 Hz. The on-axis samples were 6H-SiC and the off-axis samples were 4H-SiC. They were first degreased sequentially in acetone, methanol, and then dilute hydrogen fluoride (HF), and heated to the growth temperature in a base vacuum of 2 x 10^{-8} Torr. It should also be noted that the substrates were held in place by a pin, so there was always a small spot where no TaC was deposited, which exposed the SiC to the GaN growth process.

To establish the temperature at which the TaC should be deposited, we examined films grown at a specific temperature before and after they were annealed at elevated temperatures. We recorded θ–2θ XRD scans and Debye ring patterns for the TaC films using a Bruker General Area Detector Diffraction System (GADDS) x-ray system to determine to what extent the film was textured, and examined the surface morphology using SEM and AFM. We annealed some of the samples in an radio frequency (RF) heated furnace for 30 min at 1200, 1400, or 1600 °C and reexamined them. Cross-sectional and planar TEM and HRTEM micrographs were taken of selected samples to examine the TaC/SiC interface and assess the film's crystallinity and grain size. We also recorded selected area diffraction (SAD) patterns to determine the orientation relationship of the grains to determine to what extent the films grew epitaxially.

Using MOCVD, we grew GaN films in an Emcore reactor on TaC substrate films that had been previously deposited on 3° off-axis SiC substrates and annealed at 1600 °C. The substrates were organically cleaned and etched just prior to being loaded into the reactor. In some instances the substrate was preheated in H_2 and NH_3 for 3 min to try to remove some of the surface C and nitride the Ta, which is what we do to form Al-N bonds when we grow GaN films on sapphire.

We also grew films without nitriding with NH_3 and without either cleaning with H_2 or nitriding the surface. Films were also grown with GaN or AlN buffer layers deposited at 500 or 600 °C. All of the GaN films were grown at 1080 °C for 10 to 60 min.

We also recorded θ-2θ scans and Debye ring patterns for the GaN/TaC/SiC samples to determine to what extent the GaN films were textured, and we took (0004) GaN/ (222) TaC/ (0008(12)) SiC rocking curves using a Bede triple crystal x-ray system to measure the crystal quality of the films. (The peaks in the (0002)/(111)/(0004(6)) rocking curves were too close together to clearly distinguish them.) Next, we studied the morphology of the film using SEM and AFM, and performed cross sectional TEM and HRTEM to analyze the morphology and structure of the GaN and TaC films and their interfaces, and determine the grain size and crystal quality. Finally, we used SAD to investigate the film's orientation and its epitaxial relationship to the substrate taken. We also determined the dislocation concentration in the GaN films by counting etch pits created by etching the samples for 4 min at 480 °C in molten potassium hydroxide (KOH).

3. Results and Discussion

The SEM micrographs in figure 3 of the as-deposited TaC films grown at 600, 800, and 1000 °C show that all of them have a relatively smooth morphology. However, when they are annealed at 1600 °C, all the films, except for the one deposited at 1000 °C, break up and form individual grains shaped somewhat like spheres that are separated from each other. This indicates that the adhesion between the substrate and the film is not good because good epitaxy has not occurred, and the films deposited at the lower temperatures were further from their equilibrium structures so that the driving force for nucleation and grain growth was larger. That the films deposited at the lower temperatures are further from their equilibrium structure is also supported by the θ–2θ scans, given that the x-ray peaks were broader for the films deposited at the lower temperatures. The focus for the rest of the report will be on films grown at 1000 °C or above.

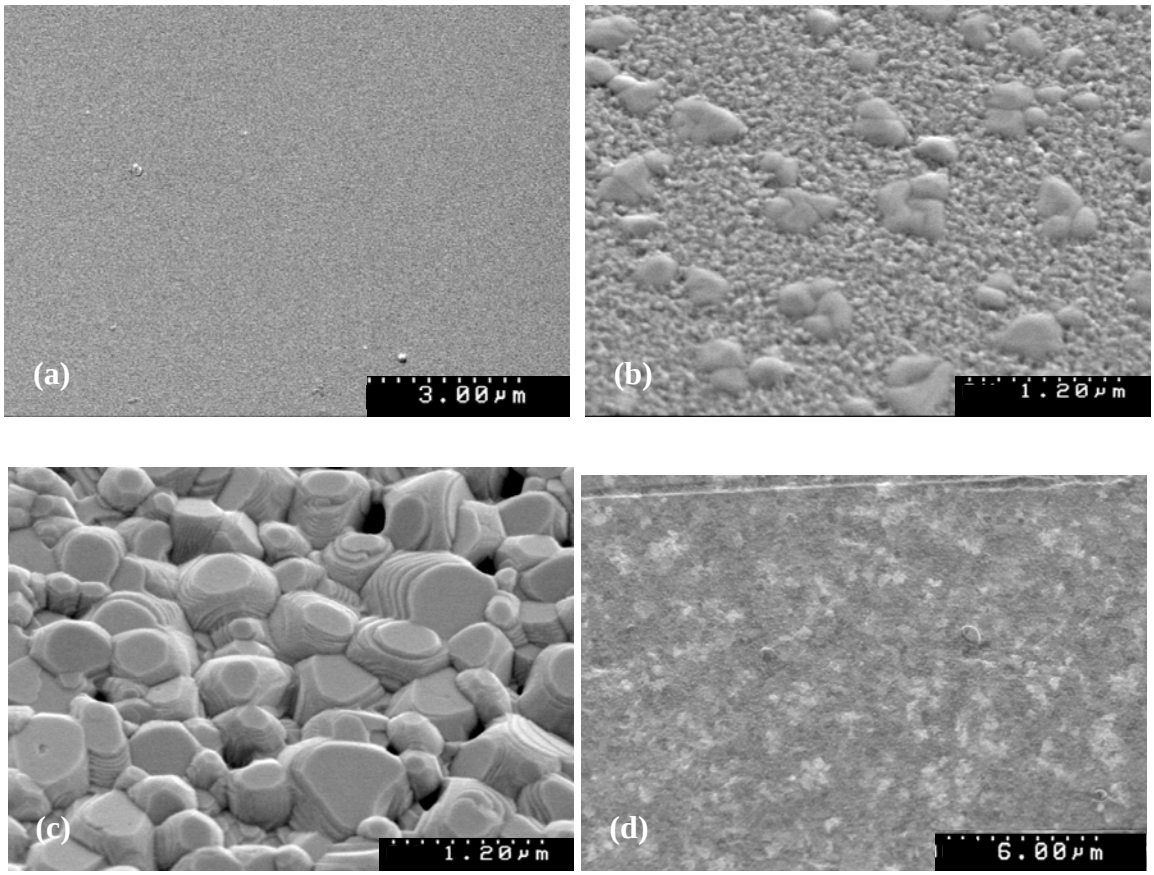

Figure 3. SEM micrographs of TaC films (a) as-deposited at 800 °C, (b) deposited at 800 °C and annealed at 1200 °C, (c) deposited at 800 °C and annealed at 1600 °C, and (d) deposited 1000 °C and annealed at 1600 °C.

The SEM micrographs in figure 4 for a TaC film deposited on an on-axis substrate at 1000 °C show that the film that looks relatively smooth at low magnification (figure 3a) has a distinct grain structure at higher magnification and the grains have a diameter of ~200 nm (figure 4a). Also, as shown in figure 4b, there were a few regions with ~200 nm diameter micropores, but there were very few of them showing that the coverage was very good. The as-deposited and annealed films looked qualitatively the same, but the grain structure was more distinct in the annealed films, suggesting that recrystallization occurs during the anneal. Also, the morphology of films grown off-axis was similar to those grown on-axis.

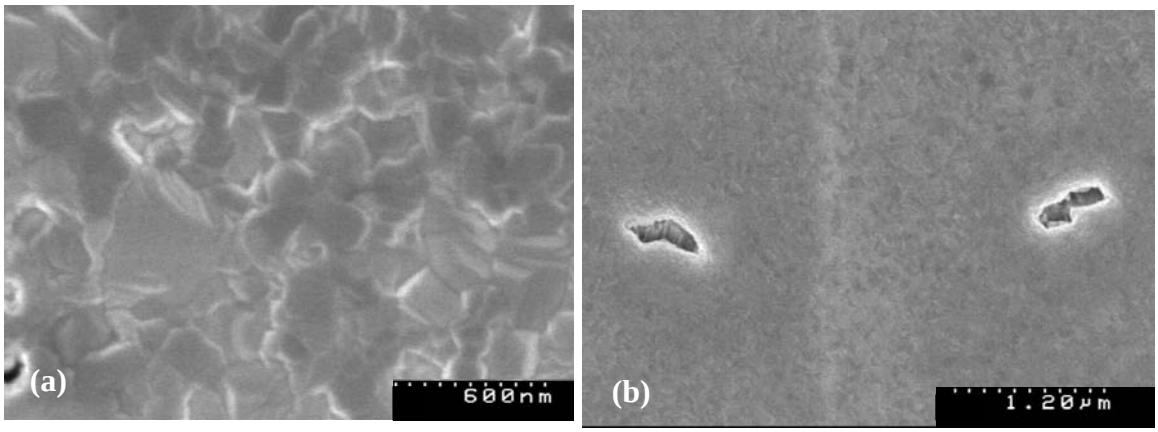

Figure 4. SEM micrographs of a TaC film deposited on an on-axis substrate at 1000 °C taken (a) at a high magnification and (b) in a region where micropores were observed.

That there is some recovery during the anneal is supported by the 5 x 5 µm AFM images in figure 5, which illustrate the morphologies of an as-deposited film and one that was annealed at 1400 °C; both were deposited at 1000 °C. What appear to be grain boundaries are much more clearly defined in the annealed film. Also, the annealed film is rougher with an rms roughness of 20.579 nm compared to 15.265 nm for the as-deposited film.

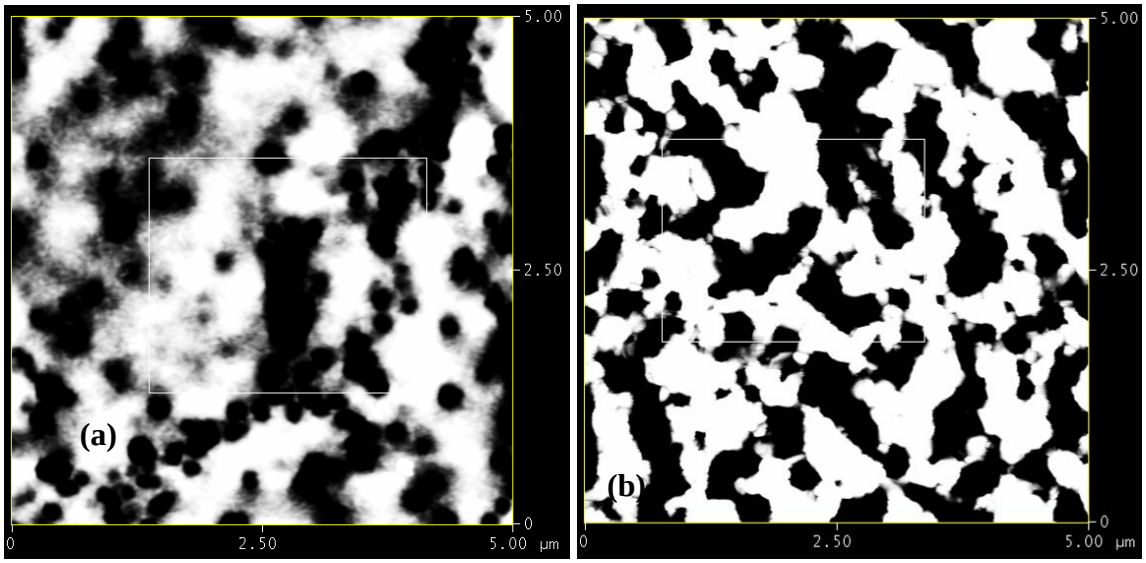

Figure 5. The 5 x 5 µm AFM micrographs of TaC films deposited on an on-axis substrate at 1000 °C, showing (a) an as-deposited film and (b) a film that was annealed at 1400 °C.

In figure 6, the θ–2θ scan of a TaC film deposited at 1000 °C on an on-axis SiC substrate shows that the film is polycrystalline, since all of the primary peaks for a randomly oriented powder sample are present. However, there is some texturing of the film as is evidenced by the fact that the basal plane reflections are more intense than those predicted for a random powder pattern as represented by the height of the solid lines, and the lines for the other reflections are larger.

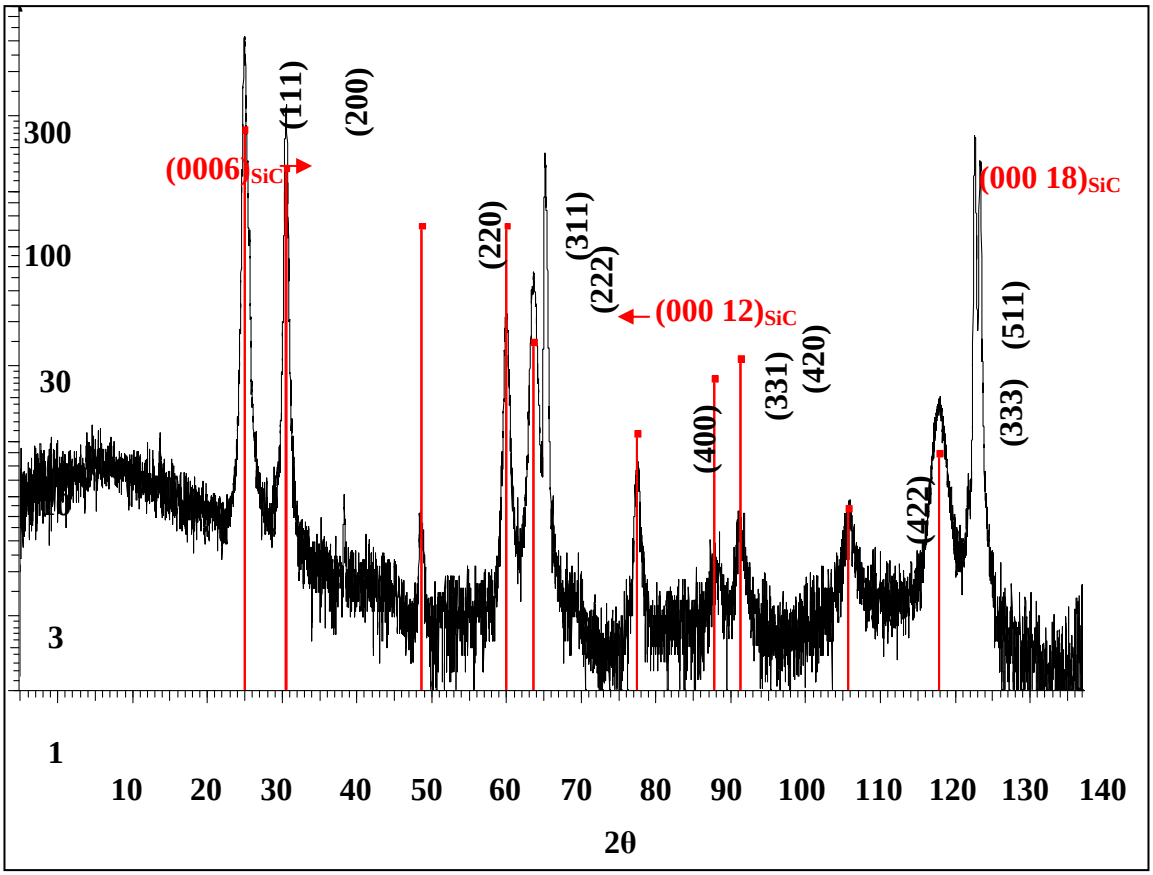

Figure 6. A complete θ–2θ scan for a TaC film deposited at 1000 °C on an on-axis 6H-SiC substrate.

As shown in figure 7 where the θ–2θ scans in the vicinity of the (a) (111) and (b) (222) TaC peaks are displayed, annealing the film at 1600 °C has little to no effect on the degree of texturing in this on-axis film. The relative intensity of the (200) TaC peak near the (111) and the (311) peak near the (222) changes very little, indicating that grains with one orientation do not grow at the expense of others as sometimes occurs during recrystallization; the same can be said for the basal plane peaks. Note also that the (0006) SiC peak cannot be distinguished from the (111) TaC peak, but the (000 12) SiC peak can be distinguished from the (222) TaC peak as now the peak separation is 2.043°.

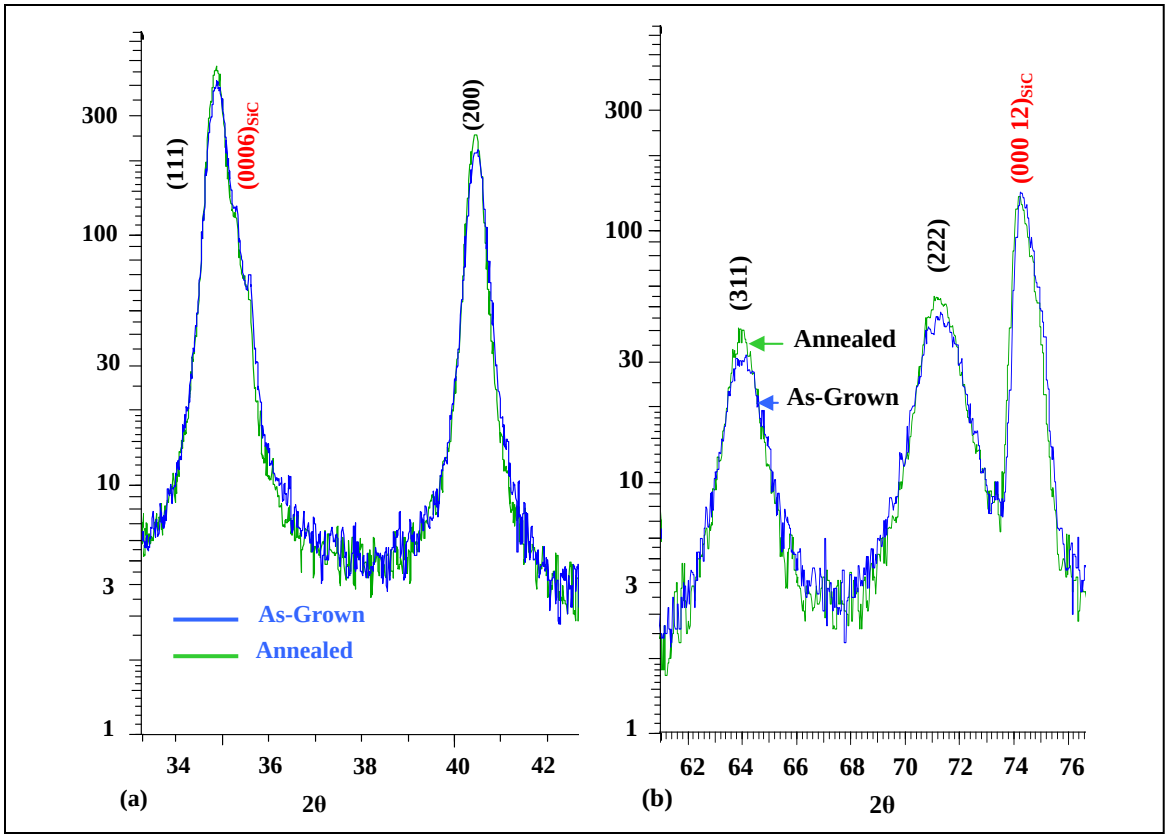

Figure 7. The θ–2θ scan for a TaC film deposited at 1000 °C in the vicinity of the (a) (111) TaC peak and (b) the (222) peak for the as-deposited and annealed films.

Films grown on 3° or 8° off-axis SiC substrates to try to promote the epitaxial relationship also do not have a 100% (111) texture, as is shown in figure 8 where the θ–2θ curves in the vicinity of the (111) or (222) TaC peaks are plotted along with those for the on-axis sample. As seen in figure 8a and 8b, the peaks for the as-deposited films of the off-axis substrates are broader, with the peaks for the 8° off-axis crystal being the broadest. In addition, there are extra peaks near 33.8° and 35.4°, which are near the $(10\bar{1}0)$ (33.32°) and (0002) (36.36°) peaks for Ta_2C. Both peaks are present in the 8° off-axis film, but only the 33.8° peak is present in the 3° off-axis film, and it is much smaller. Given that TaC has a large solubility limit for vacancies, as TaC is the equilibrium phase between 4350% C, it is also possible these peaks are associated with a metastable phase comprised of ordered C vacancies. Whatever they are, they essentially disappear in the sample annealed at 1600 °C, as shown in figure 8c and 8d. This suggests that performing these steps on the off-axis wafers impedes the diffusion of the atoms to their equilibrium positions, and the structure of the 8° off-axis samples is further from equilibrium than the 3° off-axis samples or the on-axis samples. However, after the samples have been annealed at 1600 °C, they are all quite similar as, in addition to the two extra peaks essentially disappearing, the peaks have become much sharper. The Debye ring patterns, shown in figure 9, also show that the grains in the TaC film recover during the 1600 °C anneal, given the rings in the as-deposited 3° off-axis film are more diffuse than those for the film after it has been annealed.

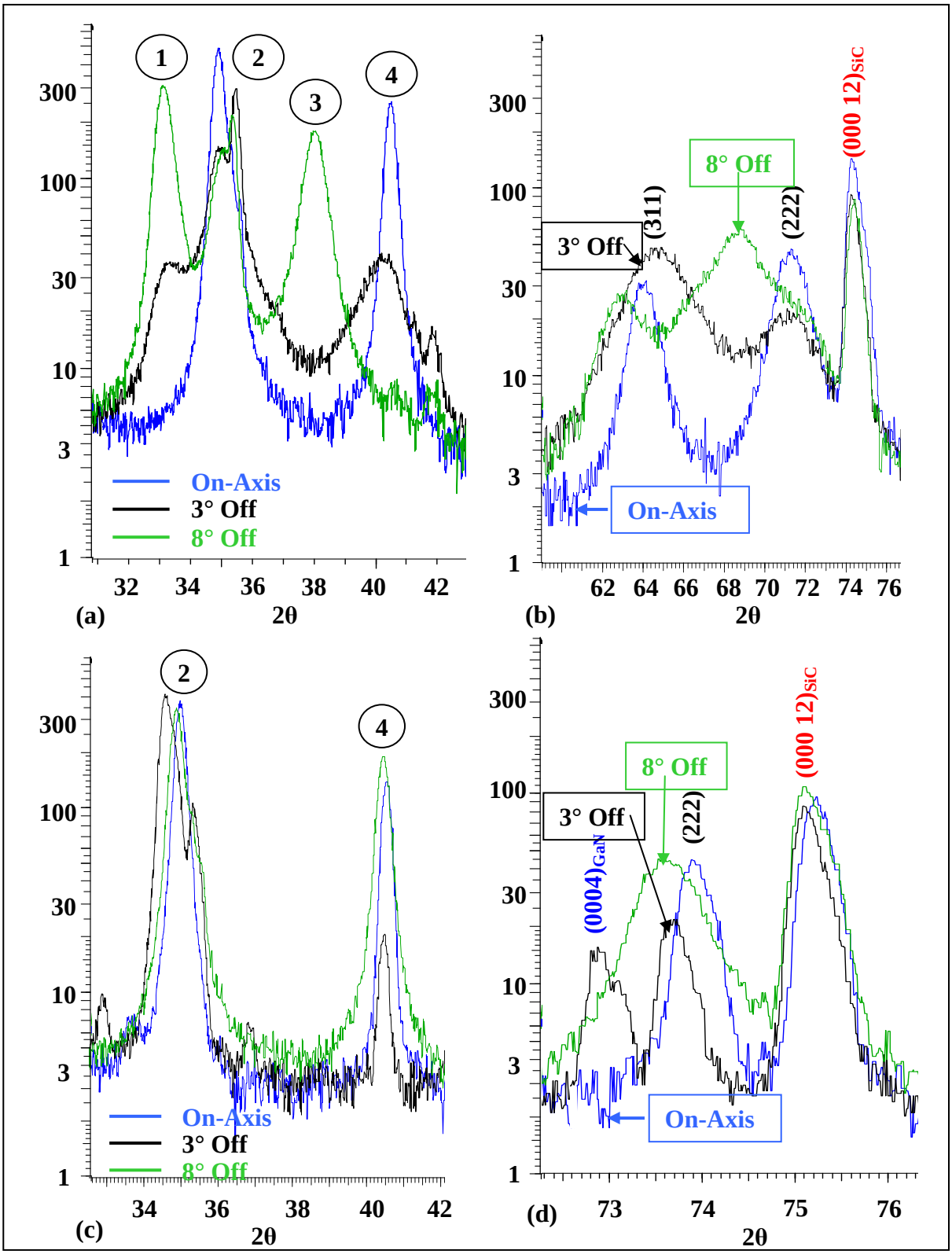

Figure 8. The θ–2θ scan for TaC films as-deposited at 1000 °C in the vicinity of (a) the (111) TaC peak and (b) the (222) peak for the on on-axis, 3° off-axis, or 8° off-axis films. The θ - 2θ scan for TaC films as-deposited at 1000 °C and annealed at 1600 °C in the vicinity of (c) the (111) TaC peak and (d) the (222) peak for the on-axis, 3° off-axis, or 8° off-axis films. Peaks 1 and 3 are extra peaks that could be associated with Ta_2C; the $(0002)_{GaN}$, $(111)_{TaC}$ and $(0006)_{SiC}$ peaks lie in region 2; and 4 is the $(200)_{TaC}$ peak.

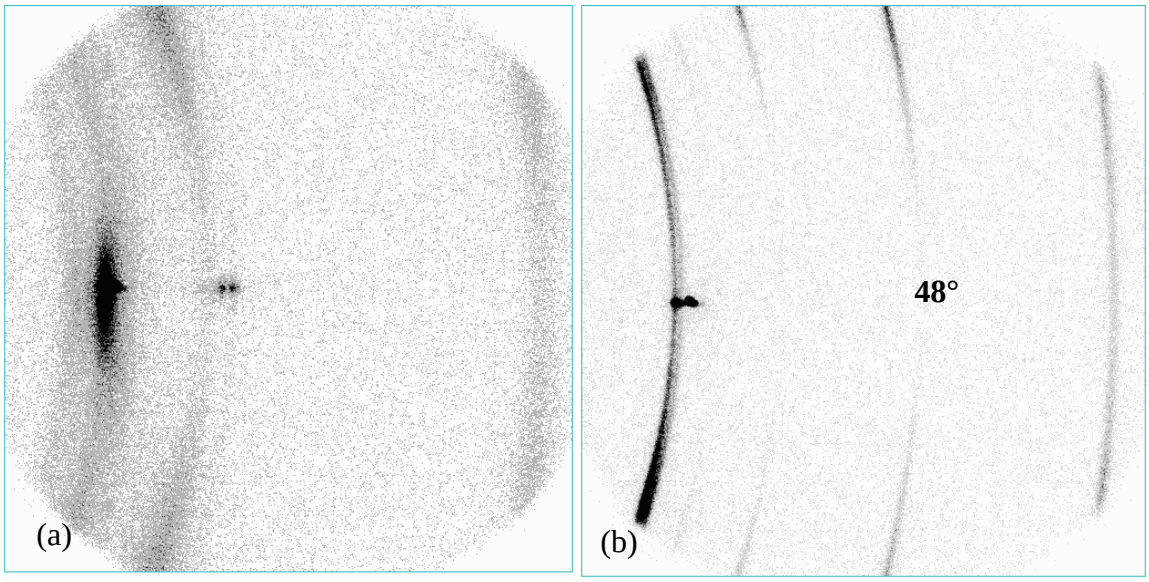

Figure 9. The Debye ring pattern for the TaC film deposited at 1000 °C on a 3° off-axis substrate: (a) as-grown and (b) annealed at 1600°C with a GaN film grown on top of it.

Note there is an extra peak near 73° in the annealed 3° off-axis sample in figure 8d. This is the $(0004)_{GaN}$ peak, which can be separated from the $(222)_{TaC}$ peak at this high angle because the peaks are separated by 0.381°. Also note in figure 9 that there appear to be two rings at 35° and an extra ring at 48°. The former is due to the $(0002)_{GaN}$ reflection and the latter is due to the $(10\bar{1}2)_{GaN}$ reflection from the GaN grown on top of the TaC film. We will return to the GaN films later.

In an attempt to obtain better epitaxy, we tried to grow the TaC films at a higher temperature, but the film became somewhat mottled, indicating that the TaC had reacted with the SiC. The contrast at the TaC/6H-SiC interface for a TaC film deposited at 1100 °C reveals the initial stages of such interfacial reactions, as shown in the cross-sectional TEM in figure 10a. The associated SAD pattern in figure 10b also demonstrates that TaC has a tendency for a predominant orientation, i.e., texture, where the (111) planes of the TaC tend to orient parallel to the *c*-planes of the 6H-SiC substrate. However, there is evidence from the SAD pattern, that the (200) TaC planes from some of the grains also tend to align parallel to the (000l) 6H-SiC planes, as well. Thus, the texturing is due, in part, to the $(111)_{TaC}$ grains having the desired epitaxial orientation relationship $(111)_{TaC} \parallel (0002)_{SiC}$ and $[10\bar{1}]_{TaC} \parallel [2\bar{1}\bar{1}0]_{SiC}$ and $[\bar{1}10]_{TaC} \parallel [\bar{1}2\bar{1}0]_{SiC}$. The TEM data from the TaC film grown at 1100 °C show that the interface has begun to roughen slightly, most probably because the TaC is reacting with the SiC. The most probable product is $TaSi_2$ because it is the phase in equilibrium with both SiC and TaC according to the Ta-Si-C ternary phase diagram (*8*). Given that these three phases (TaC-SiC-$TaSi_2$) are supposed to be in equilibrium, it is not clear what the driving mechanism would be. It is not likely that the Ta arrives in its elemental form or as a more complex carbide, as mass spectrometry of the ablated target had indicated that the only species present was Ta-C (*12*). These molecules

could, however, arrive with kinetic energy that could be dissipated through a chemical reaction with the surface (*12*). $TaSi_2$ is also the silicide formed when TaC reacts with Si to form $TaSi_2$ and SiC (*13*).

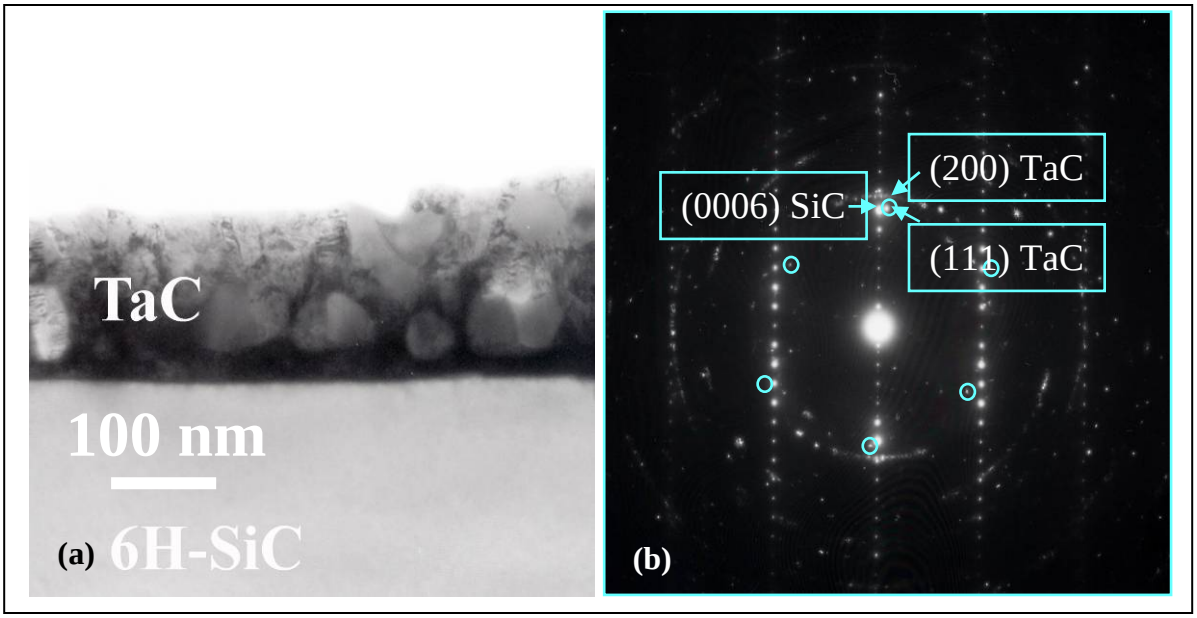

Figure 10. (a) Cross section TEM micrograph of a TaC film grown at 1100 °C, and (b) the associated SAD pattern from a region near the TaC/6H-SiC interface.

The cross section TEM microscopy of a film grown at 1200 °C displayed in figure 11a shows that the reactions at the interface are even more severe at the higher growth temperature. The HRTEM in figure 11b shows that the reaction tends to occur along crystal planes, much like it does during some etching processes. The HRTEM micrograph in figure 11c shows that the product of the interfacial reaction are elongated grains protruding vertically through the TaC/6H-SiC interface, sometimes to a depth of 100 nm into the SiC substrate, and leaving an amorphous region adjacent to the interface. The TaC film reveals a tendency for a texture, where the (002) TaC planes tend to align parallel to the (0006) SiC plane, as shown from the SAD pattern in figure 11d.

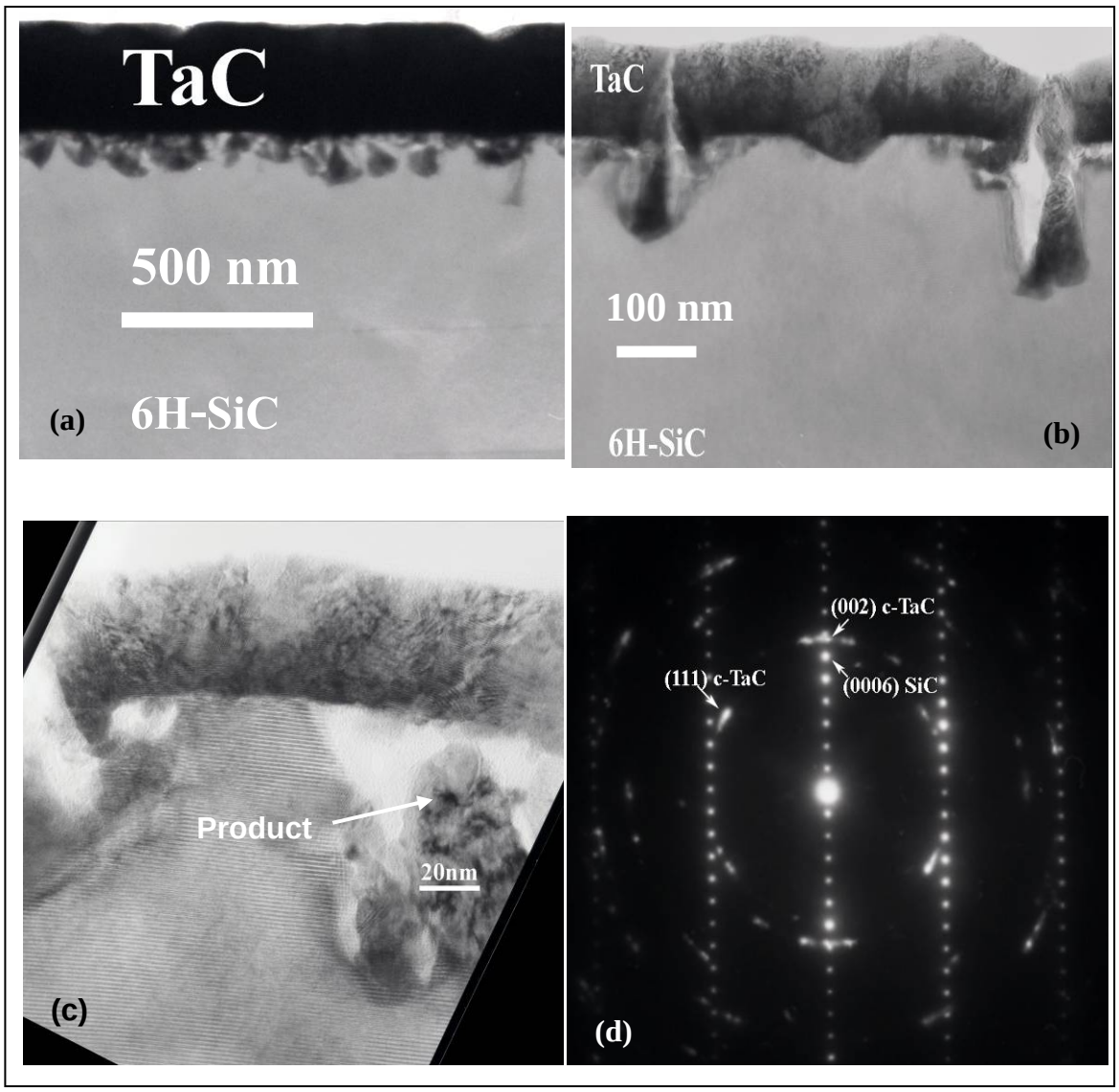

Figure 11. (a) Cross section TEM micrograph of a TaC film grown at 1200 °C, (b) HRTEM of the same region, (c) HRTEM micrograph of a reaction product at the interface, and (d) SAD pattern of the associated area.

The SEM micrographs in figure 12 reveal that GaN films can be deposited on the TaC/SiC substrate if it has been nitrided with NH_3 at 1100 °C, and an AlN buffer was used. Without the nitridation step or when a GaN buffer was used, the GaN was only deposited at selective spots on the substrate. Even when the TaC is nitrided and an AlN buffer is used, the GaN only grows on it reluctantly. This can be seen in figure 12b where the GaN that is deposited on the exposed SiC spot, the "spot" where the wire sample holder was placed during the PLD deposition of the TaC, is thicker than the GaN deposited on the TaC next to it. For films grown for shorter times so that the TaC was not totally covered by the GaN, there was a ring around the SiC spot on which very

few GaN grains had been deposited relative to regions further away from the spot. This suggests that the Ga and/or N species are much more mobile on the TaC, so that those that land on the TaC near the SiC spot diffuse to it.

Another possible explanation for the slow growth is that the GaN is deposited with the N side up, something that often occurs during MBE growth (*5*), and the growth is much slower. That this is possibly the case is illustrated in figure 12c for a 10-min growth so that the TaC does not completely cover the SiC substrate. A number of the grains that have nucleated and begun to grow have flat tops, which is indicative of N-face growth. It is also possible that there was slower growth because all of the GaN crystallites were not oriented in the fast growing [0001] direction, which would have been the case had there been perfect epitaxy. It is quite apparent that the crystallites, which are unusually large with diameters of over 1 μm, grow in many different directions in the micrograph in figure 12a. This can account for the large difference in the rms surface roughness, which was determined by AFM to be 2.94 for growth on the SiC surface, and almost 50 times larger for growth on the TaC.

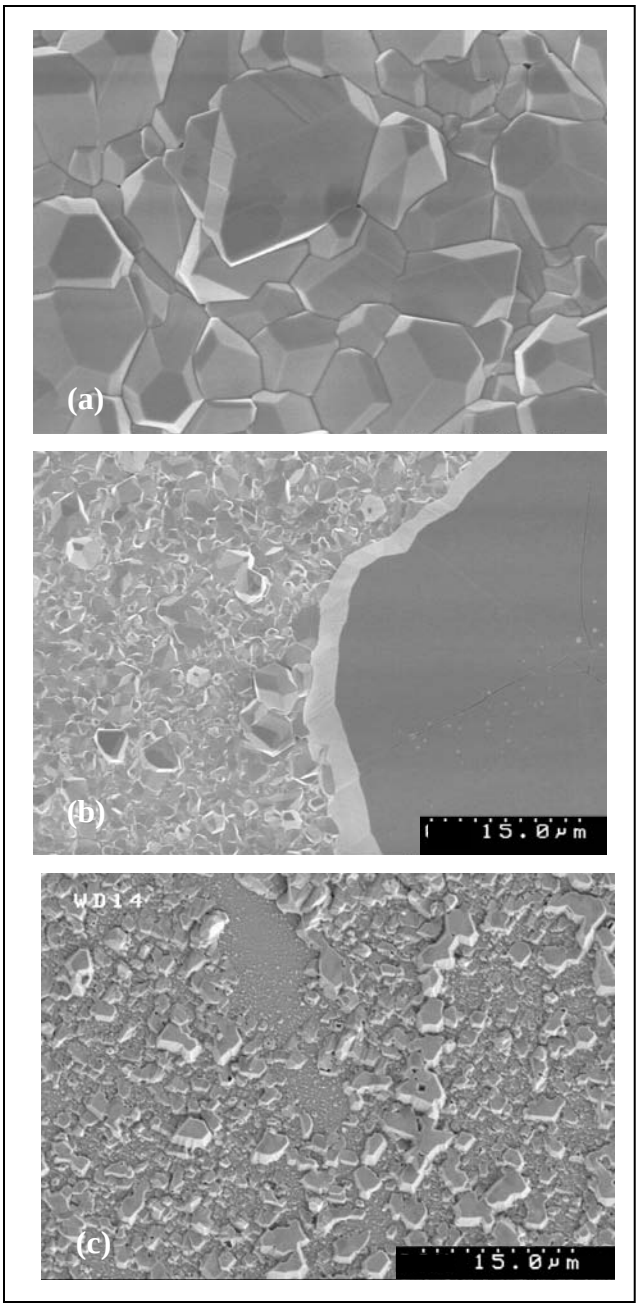

Figure 12. SEM micrographs of a GaN film grown for 45 min
(a) away from the exposed SiC spot, and (b) near it.
(c) SEM micrograph of a GaN film grown for 10 min.

That the crystallites grow in a number of different directions is confirmed in the θ–2θ scan in figure 13a. Of the seven most intense GaN peaks($10\bar{1}1$) 36.96°, ($10\bar{1}0$) 32.49°, (0002) 34.70°, ($11\bar{2}0$) 57.96°, ($10\bar{1}3$) 63.68°, ($10\bar{1}2$) 48.27, and ($11\bar{2}2$) 69.35° - only the (0002), ($11\bar{2}0$), and ($11\bar{2}2$) reflections have corresponding TaC reflections, which are the (111), ($02\bar{2}$), and ($13\bar{1}$) reflections, so they are almost superimposed on each other. The other four do not have equivalent reciprocal lattice vectors (*14*), so they should stand alone. The ($10\bar{1}1$) and ($10\bar{1}0$)

peaks are near the (111) and $(0006)_{SiC}$ peaks, so they are hard to distinguish, but they can be seen. However, the $(10\bar{1}2)$ and $(10\bar{1}3)$ are in locations of their own, and they can clearly be seen in figure 13a.

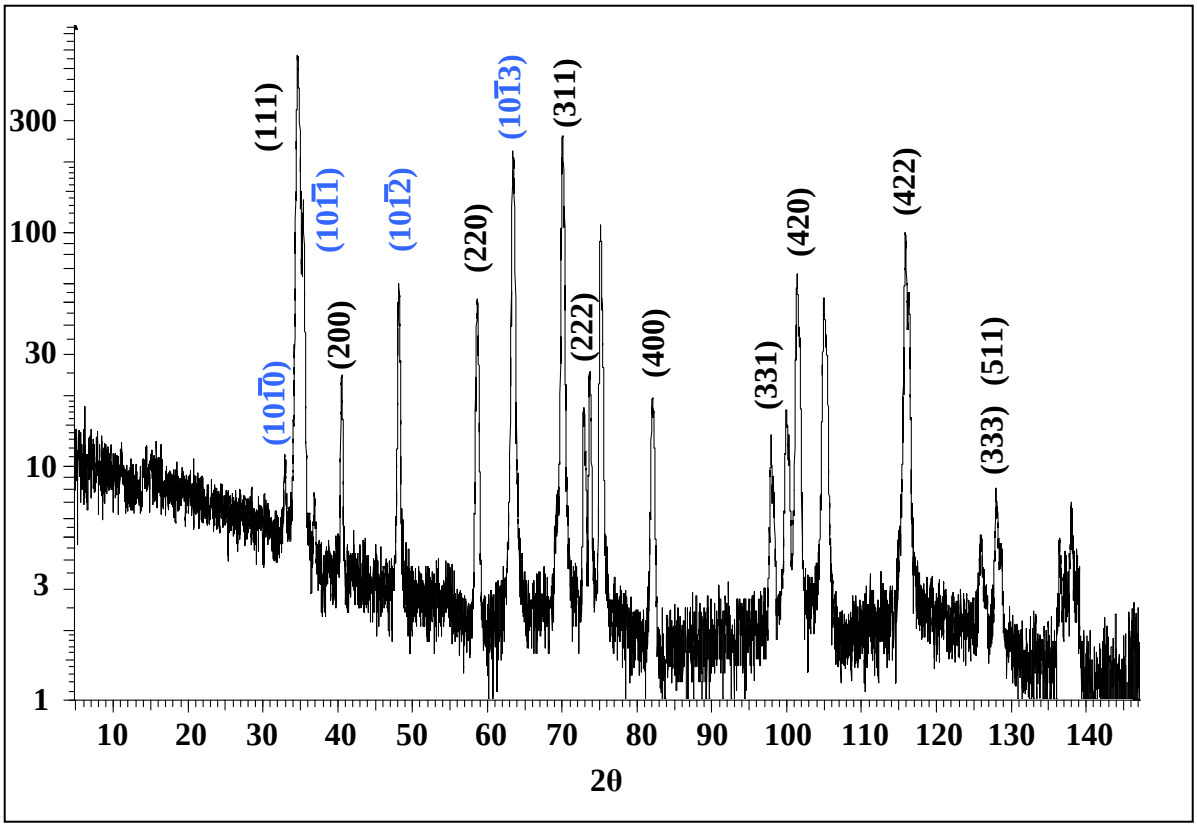

Figure 13a. (a) A complete θ–2θ scan for a GaN film grown on a TaC film deposited at 1000 °C on a 3° off-axis SiC substrate.

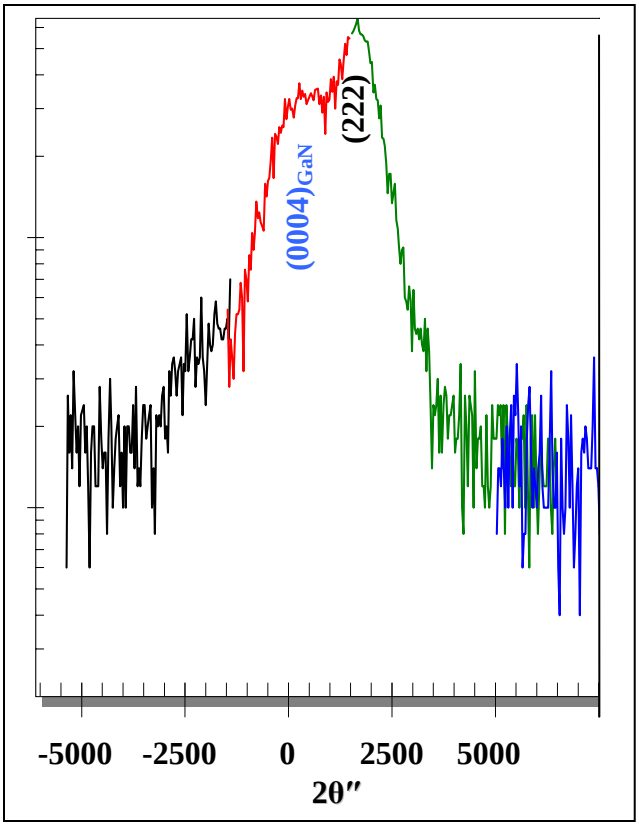

Figure 13b. Rocking curve for the $(0004)_{GaN}$ and (222) peaks.

As noted earlier in reference to figure 8d, the $(0004)_{GaN}$ peak can be distinguished from the (222) peak, even though they are corresponding planes, because of their slightly different *d*-spacings. However the $(0002)_{GaN}$ cannot be distinguished from the (111) peak. This is true even when the sample is examined using the Bede triple crystal x-ray system, because the peaks are broad and overlap with each other, as can be seen in the $(0004)_{GaN}$ and (222) rocking curves in figure 13b, where the peak widths are ~1000".

TEM analysis of the microstructure of the GaN film grown on the TaC/SiC substrate reveals that the surface of the GaN is very rough, up to ~2 μm, with individual GaN microcrystalline grains of micron to sub-micron size, leading to a non-uniform film thickness, as shown in figure 14a. One of the reasons for this high degree of roughness could be that the TaC surface itself is not very flat, but very wavy, as displayed in figure 14b. Despite that, the GaN layer has very good coverage on the TaC surface and there are no voids at the GaN/TaC interface, indicating good adhesion under these processing conditions. The individual grains are of relatively high single crystal quality, as revealed in figure 14b, and the selected area diffraction (inset) shows this grain has a *c*-axis orientation. The defects in the GaN film are mostly grain boundaries and dislocations, and stacking faults in the vicinity of the GaN/TaC interface, but the overall quality of the grains is quite good. Due to the large difference in the thickness of the three materials,

which results from the specifics of the sample preparation, the individual layers, particularly the thick TaC and SiC layers, do not show clear crystallographic details about their microstructure in the low- to mid-magnification images.

SEM micrographs of a KOH etched GaN film in figure 15 reveal that the dislocation density in the film grown on the TaC is substantially less than that grown on the SiC "spot." As seen in figure 15a, most of the etch pits in the region of the film grown on TaC are along the grain boundaries; the individual grains appear to contain very few dislocations. One can see that the total number of dislocations in the GaN grown on the TaC is less than in the GaN grown on the SiC as by comparing the number of etch pits in figures15a and 15b, which have the same magnification. Because of the surface roughness, it is difficult to quantify the dislocation density in the part of the film grown on TaC, but it is safe to say that it is more than an order of magnitude less. Using images taken at higher magnifications, such as the one shown in figure 15c, we calculated the dislocation density in the part of the film grown on the SiC to be $4 \times 10^9/cm^2$, which is what is normally found in GaN films used in most devices being made today. It appears likely that the dislocation concentration in the portion of the film grown on the TaC is $<10^8/cm^2$, which is less than what anybody else achieves for films of comparable thickness using SiC or Al_2O_3 substrates.

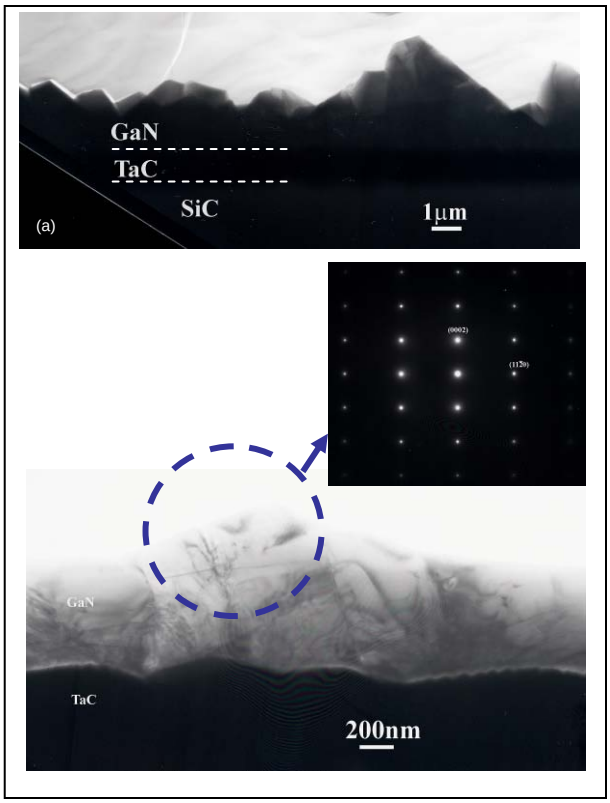

Figure 14. (a) Cross section TEM of a GaN film grown on a TaC film PLD deposited on a 4H-SiC substrate.
(b) Cross section TEM of the GaN film and its associated SAD pattern and the TaC/GaN interface.

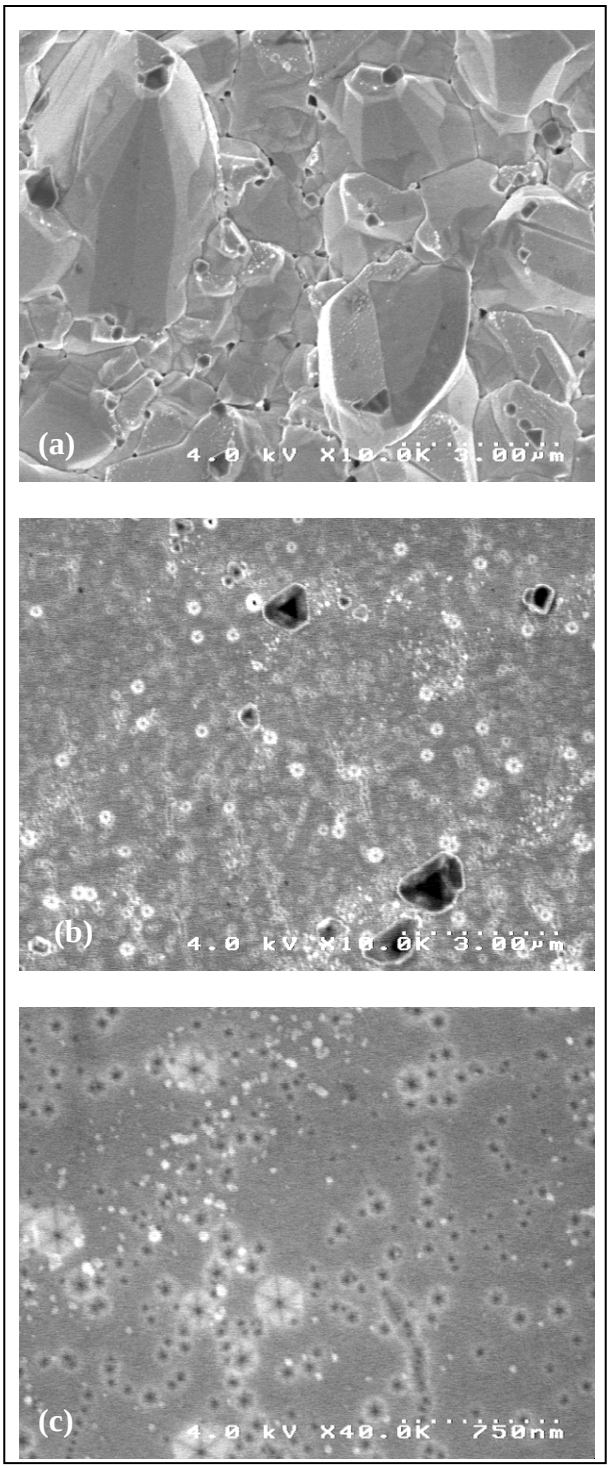

Figure 15. SEM images of GaN grown on (a) TaC and
(b) the SiC "spot" at the same magnification, and
(c) on the SiC spot at higher magnification.

4. Conclusions

Although TaC is more closely lattice matched to GaN and has a close packed structure similar to it - more similar than the frequently used Al_2O_3 substrates - we were not able to grow device quality GaN films on it, because we were unable to grow smooth TaC films with a high (111) texture. TaC films deposited at temperatures below 1000 °C do not adhere well to the SiC substrate and the grains separate from each other and form spheres when they are annealed at temperatures from 1200–1600 °C. Films deposited at 1000 °C do adhere well, but they are polycrystalline with only a slight (111) texture. TaC films deposited at higher temperatures react with the SiC substrate probably forming $TaSi_2$, even though TaC and SiC are in equilibrium with each other, as is indicated in the Ta-Si-C ternary phase diagram.

It also seems unlikely we could deposit an interlayer of Ta_2C between the SiC and TaC to break the mismatch between the TaC and SiC into two smaller mismatches that would reduce the strain energy in the TaC. This is because C from the stoichiometric TaC could diffuse into the Ta_2C and form a single phase of TaC with a large number of vacancies.

The GaN films grown on the TaC contained grains with many different orientations. As a result they were very rough because the grains with different orientations grew at different rates. These films, however, did have the advantage that they contained at least an order of magnitude fewer dislocations than is usually observed in GaN films grown to a comparable thickness. Given that the dislocation concentration in the film grown on the SiC "spot" was $4 \times 10^9/cm^2$, it is likely that the part of the same GaN film grown on the TaC had a dislocation concentration $<10^8/cm^2$, which is less than what anyone else achieves in GaN films of comparable thickness grown on SiC or Al_2O_3 substrates. Because they are of such high quality, they could be useful in fundamental optical studies.

Even though we were not able to grow highly textured TaC films with a limited number of defects, it does not mean it cannot be done. However, it will be extremely difficult to find a substrate as inert as SiC that has a similar structure and is closely lattice matched to the TaC.

5. References

1. Karpinski, J.; Jun, J.; Porowski, S. *J. Crystal Growth* **1984**, *66*, 1.
2. di Forte Poisson, M.-A.; Magis, M.; Tordjman, M.; Aubry, R.; Sarazin, N.; Peschang, M.; Morvan, E.; Delage, S. L.; di Persio, J.; Quéré, R.; Grimbert, B.; Voel, V.; Delos, E.; Ducatteau, D.; Gaquiere, C. *J. Crystal Growth* **2004**, *272*, 305.
3. Lee, C. D.; Ramachandran, V.; Sager, A.; Feenstra, R. M.; Greve, D. W.; Sarney, W. L.; Salamanca-Riba, L.; Look, D. C.; Gai, ; Song; Choyke, W. J.; Devaty, R. P. *J. Electronic Mat.* **2001**, *30*, 162.
4. Shimizu, M.; Kawaguchi, Y.; Hiramatsu, K.; Sawaki, N. *Jpn. J. Appl. Phys.* **1997**, *36*, 3381.
5. Shen, X. Q.; Ide, T.; Cho, S. H.; Shimizu, M.; Hara, S.; Okumura, H.; Sonoda, S.; Shimizu, S. *J. Crystal Growth* **2000**, *218*, 155.
6. Pierson, H. O. *Handbook of Refractory Carbides and Nitrides*; Noyes: New Jersey, 1996, Vol. 1, p. 96.
7. Pierson, H. O. *Handbook of Refractory Carbides and Nitrides*; Noyes: New Jersey, 1996, Vol. 1, p. 252.
8. Feng, J. C.; Naka, M.; Schuster, J. C. *J. Mat. Sci. Lett.* **1997**, *16*, 1116.
9. Freitas, Jr., J. A.; Rowland, L. B.; Kim, J.; Fatemi, M. *Appl. Phys. Lett.* **2007**, *90*, 09190.
10. Vispute, R. D.; Hullavarad, S.; Luyckx, A.; Young, D.; Dhar, S.; Venkatesan, T.; Jones, K. A.; Zheleva, T. S.; Ervin, M.; Derenge, M. *Appl. Phys. Lett.* **2007**, *90*, 241917.
11. Naiki, T.; Ninomiya, M.; Ihara, M. *Jpn. J. Appl. Phys.* **1972**, *11*, 1106.
12. Teghil, R.; D'Alessio, L.; Zaccagnino, M.; De Maria, G.; Ferro, D. *Appl. Sur. Sci.* **1995**, *86*, 190.
13. Laurita, T.; Molarius, J.; Kivifahti, J. K. *Microelectronic Eng.* **2004**, *71*, 301.
14. Jones, K. A. *J. Crystal Growth* **2008**, *310*, 2417.

List of Symbols, Abbreviations, and Acronyms

AFM	atomic force microscopy
AlGaN	aluminum gallium nitride
C	carbon
FCC	face centered cubic
GaAs	gallium arsenide
GADDS	General Area Detector Diffraction System
GaN	gallium nitride
HCP	hexagonal close packed
HEMTs	High electron mobility transistors
HF	hydrogen fluoride
HRTEM	high resolution TEM
KOH	molten potassium hydroxide
KrF	krypton fluoride
MBE	molecular beam epitaxy
MgO	magnesium oxide
MOCVD	metal organic chemical vapor deposition
N	nitrogen
PLD	pulse laser deposition
RF	radio frequency
SAD	selected area diffraction
SEM	scanning electron microscopy
SiC	silicon carbide
TaC	tantalum carbide
TEM	transmission electron microscopy

TiC	titanium carbide
UV	ultraviolet
XRD	x-ray diffraction

No. of Copies	Organization
1 (PDF only)	DEFENSE TECHNICAL INFORMATION CTR DTIC OCA 8725 JOHN J KINGMAN RD STE 0944 FORT BELVOIR VA 22060-6218
1	DIRECTOR US ARMY RESEARCH LAB IMNE ALC HRR 2800 POWDER MILL RD ADELPHI MD 20783-1197
1	DIRECTOR US ARMY RESEARCH LAB AMSRD ARL CI OK TL 2800 POWDER MILL RD ADELPHI MD 20783-1197
1	DIRECTOR US ARMY RESEARCH LAB AMSRD ARL CI OK PE 2800 POWDER MILL RD ADELPHI MD 20783-1197

ABERDEEN PROVING GROUND

1	DIR USARL AMSRD ARL CI OK TP (BLDG 4600)

INTENTIONALLY LEFT BLANK.